Title	Effect of remediation parameters on in-air ambient dose equivalent rates when remediating open sites with radiocesium-contaminated soil
Author(s)	Malins A., Kurikami Hiroshi, Kitamura Akihiro, Machida Masahiko
Citation	Health Physics, 111(4), p.357-366
Text Version	Author Accepted Manuscript
URL	https://jopss.jaea.go.jp/search/servlet/search?5053850
DOI	https://doi.org/10.1097/HP.0000000000000552
Right	©2016 by the Health Physics Society This is a non-final version of an article published in final form in "Health Physics, 111(4), p.357-366 (2016)".

Effect of Remediation Parameters on In-Air Ambient Dose Equivalent Rates when Remediating Open Sites with Radiocesium Contaminated Soil

Alex Malins,* † Hiroshi Kurikami,* ‡ ** Akihiro Kitamura,* ‡ ** Masahiko Machida.*

* Center for Computational Science & e-Systems, Japan Atomic Energy Agency, University of Tokyo Kashiwanoha Campus Satellite, 178-4-4 Wakashiba, Kashiwa-shi, Chiba 277-0871, Japan,

‡ Sector of Fukushima Research and Development, Japan Atomic Energy Agency, 1-29 Okitama-cho, Fukushima-shi, Fukushima 960-8034, Japan,

** Radioactive Waste Processing and Disposal Research Department, Japan Atomic Energy Agency, 4-33 Tokai-mura, Naka-gun, Ibaraki 319-1194, Japan.

† Corresponding author. Tel: +81-7135-2412. Fax: +81-7135-2382. Email: malins.alex@jaea.go.jp.

Keywords: decontamination; radioactivity, environmental; dose equivalent; soil

Conflicts of Interest and Source of Funding: AM was employed as a Hazard Management Specialist for Cavendish Nuclear between July 2012 and March 2014. This work was completed between July 2015 and January 2016. Cavendish Nuclear had no financial, editorial or scientific input to this work or the decision to publish.

ABSTRACT

Calculations are reported for ambient dose equivalent rates [$\dot{H}^*(10)$] at 1 m height above the ground surface before and after remediating radiocesium contaminated soil at wide and open sites. The results establish how the change in $\dot{H}^*(10)$ upon remediation depends on the initial depth distribution of radiocesium within the ground, on the size of the remediated area and on the mass per unit area of remediated soil. The remediation strategies considered were topsoil removal (with and without recovering with a clean soil layer), interchanging a topsoil layer with a subsoil layer, and in situ mixing of the topsoil. The results show the ratio of the radiocesium components of $\dot{H}^*(10)$ post-remediation relative to their initial values (residual dose factors). It is possible to use the residual dose factors to gauge absolute changes in $\dot{H}^*(10)$ upon remediation. The dependency of the residual dose factors on the number of years elapsed after fallout deposition is analyzed when remediation parameters remain fixed and radiocesium undergoes typical downward migration within the soil column.

INTRODUCTION

Gamma radiation from ^{134}Cs and ^{137}Cs radioisotopes dispersed by a nuclear accident, test or dirty bomb can cause elevated air dose rates for years following fallout deposition. Radiocesium has low mobility in the environment due to its tendency to bind to clay minerals within soils (Okumura et al. 2013). Remediation of soils following contamination by radiocesium is a strategy employed to lower external radiation dose rates (Jacob et al. 2001, 2009; EURANOS 2010; Ulanovsky et al. 2011; UNSCEAR 2014; IAEA 2015).

The International Commission on Radiation Units and Measurements (ICRU 1993) recommends measuring the operational quantity *ambient dose equivalent* in areas where external irradiation may occur. The ambient dose equivalent [$H^*(d)$] is defined as the dose equivalent that would be produced at a depth d (mm) in the ICRU sphere phantom on the radius opposing the direction of the corresponding expanded and aligned radiation field to the true external field. The ambient dose equivalent can be used to limit radiation protection quantities, which cannot be measured directly (e.g. the *effective dose*), to persons spending time within external radiation fields (ICRP 2007). A depth $d = 10$ mm [$H^*(10)$] is recommended for limiting the effective dose in strongly penetrating external fields, such as the gamma-rays from ^{134}Cs and ^{137}Cs decay.

In the context of environments contaminated with radio-cesium fallout, the *ambient dose equivalent rate* [$\dot{H}^*(10)$] is monitored at a height of 1 m above the ground surface. $\dot{H}^*(10)$ at 1 m provides a conservative estimate of the effective dose rate to persons within environmental fields (Satoh et al. 2016), hence it can be used to limit the yearly effective doses to people living or working within contaminated areas (ICRP 2009). Previously Malins et al. (2016) developed a tool to calculate ambient dose equivalent rates in areas where soil is contaminated with radiocesium. The tool was validated by using soil activity samples from Japan contaminated by the 2011 Fukushima Daiichi Nuclear accident to predict $\dot{H}^*(10)$ values, then comparing the predictions to environmental measurements taken with hand-held survey meters. One advantage of the tool is the ability to model arbitrary radiocesium distributions within the ground, thus allowing the simulation of different remediation scenarios and conditions.

Remediation of radiocesium contaminated soil is difficult because gamma rays from contamination spreading over hundreds of meters contribute significantly to the 1 m ambient dose equivalent rate (Malins et al. 2015). This paper presents new modelling results evaluating systematically how the change in $\dot{H}^*(10)$ upon remediation depends on the initial distribution of radioactive cesium with soil mass depth, the type of remediation strategy and on its parameters. The remediation parameters considered were the mass depth of remediated soil

and the size of the remediation area. The results are presented as graphs showing the ratio of the ^{134}Cs or ^{137}Cs component of $\dot{H}^*(10)$ after remediation to its initial value, as functions of different initial radiocesium distributions and remediation parameters.

The results can be used to estimate the absolute change in the ambient dose equivalent rate upon remediation under different scenarios. An example application is presented where the dependency of residual dose factors upon remediation on the time elapsed since fallout deposition is established, considering fixed remediation parameters and typical downward migration of radiocesium within the soil column.

MATERIALS AND METHODS

Modelling ^{134,137}Cs-contaminated soil and $\dot{H}^*(10)$

The research employed a tool to calculate the components of $\dot{H}^*(10)$ (μSv h^{-1}) attributable to ^{134}Cs and ^{137}Cs within soil (Malins et al. 2016). The ambient dose equivalent rate in radiocesium contaminated areas is broken down as

$$\dot{H}^*(10) = {}^{134}\dot{H}^*(10) + {}^{137}\dot{H}^*(10) + {}^{nat}\dot{H}^*(10), \quad (1)$$

where $^{134}\dot{H}^*(10)$ (μSv h^{-1}) and $^{137}\dot{H}^*(10)$ (μSv h^{-1}) are the components due ^{134}Cs and ^{137}Cs respectively, and $^{nat}\dot{H}^*(10)$ (μSv h^{-1}) is the background component due to natural ^{40}K and uranium and thorium series radionuclides.

The tool models a half-space geometry, where a flat plane representing the ground separates regions of soil and air (ICRU 1994). The soil is split into separate cells by a regular grid. The soil blocks are 12.5 by 12.5 m in length and breadth and 1 mm in thickness. The geometry extends to 149 by 149 cells in the horizontal directions (1862.5 by 1862.5 m) and 500 soil layers in depth, equating to a maximum soil mass per unit area of 80 g cm^{-2}. These dimensions are sufficiently large to converge the calculations for $\dot{H}^*(10)$.

^{134}Cs and ^{137}Cs activity concentrations (Bq m^{-3}) can be set independently within all soil cells on the mesh. Conversion factors (units of μSv h^{-1} per Bq m^{-3}) relate the activity concentrations to their contribution to $^{134,137}\dot{H}^*(10)$ at 1 m height above the central cell on the mesh. The conversion factors were calculated using the Particle and Heavy Ion Transport code System (PHITS - ver. 2.64) Monte Carlo radiation transport code (Sato et al. 2013). The elemental compositions of soil and air in the Monte Carlo simulations followed Eckerman and Ryman (1993), and the densities were 1.6 g cm^{-3} and 0.0012 g cm^{-3} respectively. The conversion factors are applicable for other soil densities when the radiocesium source distribution is expressed as a function of soil mass per unit area (Saito and Petoussi-Henss 2014).

$^{134,137}\dot{H}^*(10)$ were calculated by summing the product of the activity concentration and the activity-dose conversion factor for all soil cells on the mesh. The relative standard deviation of the calculation results due to Monte Carlo statistical uncertainty in the conversion factors was always lower than 0.5%.

The use of the half-space geometry means that the results are most applicable for remediating flat, wide and open locations with unpaved surfaces and low lying vegetation. In reality there will always be deviation from this ideal case. Malins et al. (2016) discuss the validity of the modelling geometry, and good correlation was found between predictions using the tool and survey meter measurements at various contaminated sites in North-East Japan, including agricultural land and public parks. Although the applicability of the results presented in this paper is limited to such settings, remediating contaminated soil at open locations can incur large financial costs. For example, Yasutaka et al. (2013) calculated that the cost of remediating the agricultural land within the special decontamination area of Fukushima Prefecture after the 2011 Fukushima Daiichi Nuclear accident was up to 80% of the total cost for the whole area. Therefore it is important to study the relationship between remediation parameters and dose rate reductions at open sites with radiocesium contaminated soil.

Initial distribution of radiocesium

Soil samples taken at undisturbed, open locations in Eastern Europe following the Chernobyl nuclear accident and in Japan following the Fukushima accident have revealed two characteristic distributions for radiocesium with soil mass depth (Likhtarev et al. 2002; IAEA 2008; Matsuda et al. 2015). At some locations the radiocesium activity concentration of the soil decreases continuously with increasing depth below the surface. These depth profiles are commonly fitted by an exponential function of the form

$$A_n(\zeta) = A_{n,0} \times \exp(-\zeta/\beta), \quad (2)$$

where $A_n(\zeta)$ (Bq m^{-3}) is the depth-dependent activity concentration, and $A_{n,0}$ (Bq m^{-3}) is the activity concentration at the surface. The subscript n denotes either ^{134}Cs or ^{137}Cs. Within the exponential term, β (g cm^{-2}) is the relaxation mass per unit area, which is a parameter that characterizes the penetration of radiocesium fallout into the ground. ζ (g cm^{-2}) is the mass of soil per unit area intervening between the surface and a physical depth of z (cm) beneath the surface (ICRU 1994),

$$\zeta(z) = \int_0^z \rho_s(z)\mathrm{d}z, \quad (3)$$

where $\rho_s(z)$ (g cm^{-3}) is the soil density, which can also vary with depth. Activity distributions in the soil column are characterized as functions of soil mass per unit area rather than physical

depth, as ζ quantifies the amount of the shielding provided by the soil (Saito and Petoussi-Henss 2014).

A second type of radiocesium activity distribution that is commonly observed displays a peak in the activity concentration below the surface (Likhtarev et al. 2002; Matsuda et al. 2015). Matsuda et al. (2015) proposed a hyperbolic secant distribution as a fitting function for these profiles, as this function can reproduce the peak in activity concentration below the surface before tending to the exponential distribution at large mass depths. The function is

$$A_n(\zeta) = A_{n,0} \times \cosh(-\zeta_0/\beta) \times \sinh[(\zeta_0-\zeta)/\beta], \quad (4)$$

where ζ_0 (g cm^{-2}) is the soil mass per unit area of the activity peak below the ground surface. The parameters $A_{n,0}$ and β are as per Eq. 2.

Both the exponential and hyperbolic secant functions were used to model the initial activity distribution of ^{134}Cs and ^{137}Cs within the ground prior to remediation. A homogenous distribution of activity across the full area of the model (1862.5 by 1862.5 m) was assumed in all cases. The parameters β and ζ_0 were adjusted to characterize different stages of radiocesium migration within the soil column in the months and years following fallout deposition.

Remediation strategies for contaminated soil

The remediation strategies modelled were topsoil removal with and without replacement by a clean covering soil, interchanging a topsoil layer with a subsoil layer, and topsoil mixing. The strategies are abbreviated as A1-A4, following Yasutaka et al. (2013) and Yasutaka and Naito (2016). Table 1 shows representative ranges of the remediation masses per unit area for the four remediation strategies when employed as a countermeasure on radiocesium contaminated land (JAEA 2015).

For modelling purposes it is necessary to define a post-remediation distribution for the activity concentration with soil mass depth. The post-remediation distributions used are shown in Fig. 1. Square remediation plots were modelled and the change in $^{134,137}\dot{H}^*(10)$ upon remediation calculated at 1 m above the center of the remediation plot.

In the topsoil removal strategies (A1 and A2), any vegetation covering the surface is first cut back and removed. The topsoil is then stripped away mechanically to a pre-specified soil remediation mass per unit area. A fixing agent may be applied onto the ground to assist topsoil stripping. The stripped topsoil is then collected and packed into heavy duty bags, before being transported off-site for ultimate disposal as radioactive waste (JAEA 2015). The stripped land surface may either be recovered with a fresh topsoil layer clean of contamination (A1) or left in its bare state (A2).

The post-remediation activity distribution for strategy A1 is zero activity within the replacement surface layer followed by the original activity distribution at larger mass depths (Fig. 1, blue line). This profile assumes equal masses of the stripped and replacement soil. For A2, the post-remediation distribution is the original distribution for mass depths beneath the stripped topsoil layer (Fig. 1, yellow line).

In the layer interchange remediation method (A3) a mechanical digger first excavates and collects a layer of topsoil. A second layer of soil with identical thickness (approximated as identical mass) is excavated from the pit that has been created. The pit is refilled first with the original topsoil layer, and then levelled to the ground surface with the layer that was originally subsoil. The post-remediation activity distribution assumes that the activity within the original topsoil layer is mixed homogeneously by the processes of stripping then refilling into the pit. Likewise the activity of the original subsoil layer is mixed homogeneously as it is excavated and used to recover to the ground surface. Thus the activity concentration takes two constants within the swapped layers after remediation, equal to the mean activity concentrations in each of those layers prior to remediation. The distribution below remains unchanged (Fig. 1, green line). The remediation mass per unit area for A3 is defined as the total mass per unit area of the interchanged layers.

The final remediation method considered was mixing of the soil nearest the ground surface to a specified remediation mass per unit area (A4). This can be achieved by ploughing or rotovating the soil (JAEA 2015). An assumption of homogeneous spread of activity within the mixed soil upon completion was used to derive the post-remediation activity concentration profile (Fig. 1, red line).

Residual dose factors

The results are presented as graphs showing the ratio of the ^{134}Cs or ^{137}Cs component of $\dot{H}^*(10)$ after remediation relative to its initial value prior to remediation, i.e.

$$R_{134} = {}^{134}_{r}\dot{H}^*(10) \,/\, {}^{134}_{i}\dot{H}^*(10), \tag{5}$$

$$R_{137} = {}^{137}_{r}\dot{H}^*(10) \,/\, {}^{137}_{i}\dot{H}^*(10), \tag{6}$$

where subscripts i and r correspond to initial and remediated states respectively.

R_{134} and R_{137} are termed *residual dose factors*. Residual dose factors less than 1.0 correspond to a reduction in $^{134,137}\dot{H}^*(10)$ by remediation, and greater than 1.0 to an increase.

Depth distribution with years elapsed post-fallout

At undisturbed sites radiocesium tends to migrate downwards in the soil column over the

years following fallout due to weathering and other environmental factors. This is reflected in increases in the relaxation mass per unit area (β) of the exponential distribution, and β and ζ_0 in the hyperbolic secant distribution, measured over time in soil cores.

ICRU 53 (1994) lists generic values of β for the exponential distribution as a function of elapsed time since fallout deposition for moderate climates (Table 2). The data are based on results from soil cores taken at weapons testing sites and sites contaminated by Chernobyl fallout.

Likhtarev et al. (2002) analyzed the radiocesium distribution in soil columns taken between 1988 and 1999 at undisturbed sites in Ukraine after the Chernobyl accident. From these results, they derived an attenuation factor which characterizes the reduction in dose rates over time due to shielding within the soil column relative to a plane of radiocesium on the ground surface. The attenuation factor is

$$r_{Cs}(t) = 0.82 \times [A \times \exp(-L_1 t) + (1\text{-}A) \times \exp(-L_2 t)], \quad (7)$$

where t is the time elapsed following fallout deposition (y), and A, L_1 and L_2 are empirical parameters determined to be respectively 0.4, 0.46 y^{-1} and 0.014 y^{-1}. Table 3 lists values of the attenuation factor for up to 13 years following deposition. It also lists corresponding relaxation masses per unit area for the exponential distribution that yield an identical residual dose factors relative to a plane source.

The data in Tables 2 and 3 were used to establish how activity distributions evolving over time affect the remediation residual dose factors. An initial exponential activity distribution was varied according to the elapsed time post-fallout by adjusting the relaxation mass per unit area according to Tables 2 and 3. For the ICRU 53 data (Table 2) fast, medium and slow migration scenarios were defined based on the extremes and centers of the time ranges quoted for each β value. Residual dose factors were then calculated for a fixed size remediation area (37.5 by 37.5 m) and fixed remediation mass depths of 6.7 g cm^{-2} for strategies A1 and A2, 40.3 g cm^{-2} for strategy A3 and 33.8 g cm^{-2} for A4. These remediation mass depths correspond to remediation to a depth of 5 cm, 30 cm and 25 cm, respectively, for soil with density 1.35 g cm^{-3} (typical for Fukushima Prefecture, Japan – Matsuda et al. 2015). These depths are representative of actual remediation practice (JAEA, 2015).

RESULTS

Initial exponential activity distribution

Results are presented first for an initial radiocesium activity distribution which is exponential with soil mass depth. Figs. 2a-c show residual dose factors as a function of the

mass per unit area of remediated soil. β in the exponential distribution increases between Figs. 2a-c, corresponding to deeper fallout migration within the soil column.

Fig. 2a shows results for β = 1.0 g cm^{-2}, which is characteristic of the relaxation masses per unit area seen in the first year following a fallout event (Table 2). When comparing identical volumes of soil processed by different remediation methods (i.e. equal remediation masses per unit area), the most effective strategies for reducing dose rates are the topsoil stripping methods (A1 and A2), as they yield the lowest values of R_{134} and R_{137}.

The residual dose factors for A1 and A2 decrease rapidly on remediating the top centimeters of the surface soil. They attain plateaus for remediation masses greater than 5 g cm^{-2}, indicating that radiocesium has been essentially cleared from within the remediation plot. Further remediation of soil at larger mass depths thus confers no additional reduction in the dose rate. The residual dose rate constituting the plateau is due to radiocesium lying outside of the remediated area.

In contrast to the topsoil stripping methods, the residual dose factors achieved by the soil layer interchange (A3) and soil mixing (A4) strategies decrease more smoothly with increasing remediation mass. It takes substantially larger remediation masses per unit area for soil layer interchange or soil mixing to attain values of $R_{134,137}$ that are achieved with the topsoil stripping methods with a remediation mass per area of 5 g cm^{-2}.

The benefit of soil layer interchange and soil mixing for reducing the dose rate arises because they redistribute radiocesium deeper within the ground. Residual dose factors are conferred by an increase in the amount of shielding provided by soil. Soil layer interchange yields smaller residual dose factors than soil mixing when comparing equal values of the remediation mass. This is because layer interchange redistributes radiocesium lower into the ground than soil mixing (cf. Fig. 1).

The effect of the relaxation mass per unit area β in the initial exponential radioactivity distribution on the performance of different remediation methods is shown from Figs. 2a-c, where β increases between 1.0-5.0 g cm^{-2}. If the remediation masses per unit area remain fixed, $R_{134,137}$ increase as β increases.

When β = 1.0 g cm^{-2}, the difference in performance of topsoil stripping with and without recovering with a clean soil layer (A1 versus A2) is small (Fig. 2a). However, for larger values of β there is an interval of remediation mass values prior to $R_{134,137}$ attaining the plateaus where topsoil removal with clean soil recovering performs better than topsoil removal alone (Fig. 2c). In this interval, residual radiocesium contamination remains within the ground below the topsoil layer that is stripped away. The clean soil layer (A1) acts as a shield for this residual

radioactivity leading to smaller $R_{134,137}$ than when there is no clean soil covering layer (A2).

Effect of the area of remediated land

The effect of varying the area of land that is remediated is shown in Figs. 3a-c. The square remediation plot varies from 12.5 by 12.5 m to 637.5 by 637.5 m between the different color lines. The remediation performance rises, i.e. smaller $R_{134,137}$ are obtained, with increasing area of the remediation plot.

Fig. 3a shows results for topsoil stripping and recovering with a clean soil layer (A1). Although not shown, the results for topsoil stripping alone (A2) are quantitatively similar. The plateaus indicating near-complete removal of radiocesium from within the remediated zone decrease in height with increasing area of the zone. For a 637.5 by 637.5 m remediation area, the radiocesium component of $\dot{H}^*(10)$ drops to less than 1% of its initial value.

The results for soil layer interchange (A3) and soil mixing (A4) are shown in Fig. 3b and c, respectively. They show a similar trend in that remediating a larger area results in smaller $R_{134,137}$ values.

Initial hyperbolic secant activity distribution

Residual dose factors when the initial distribution of radiocesium within the ground is the hyperbolic secant distribution are shown in Figs. 4a-i. Both β and ζ_0 in the hyperbolic secant distribution vary between the panels.

The basic features of the results are comparable to when the initial depth distribution is exponential (cf. Figs. 2a-c) The topsoil removal methods (A1, A2) generally yield smaller residual dose factors than soil layer interchange (A3) or soil mixing (A4) when comparing identical remediation masses per unit area. $R_{134,137}$ in the topsoil stripping methods attain plateaus for sufficiently large remediation masses per unit area, indicating removal of radiocesium from within the remediation plot. In comparison, $R_{134,137}$ for soil layer interchange and soil mixing strategies change more smoothly with increasing remediation mass per unit area. Deeper initial radiocesium distributions within soil (i.e. larger β or ζ_0) generally result in larger residual dose factors when comparing equal remediation masses per unit area.

For some initial hyperbolic secant distribution parameters, remediation by methods A2-A4 can result in increased dose rates after remediation, i.e. $R_{134,137} > 1.0$. This effect is shown in Fig. 4g and h when the remediation mass per unit area is small. The explanation for this phenomenon is that the radiocesium activity peak below the surface prior to remediation is closer to the surface after remediation. The shielding provided by soil is thus lowered compared

to the initial state, and there is a corresponding increase in the dose rate. Notably this phenomenon does not occur for the topsoil stripping and recovering method (A1), as the shielding that was provided by the stripped topsoil layer is replaced by the clean soil covering layer. By increasing the remediation masses per unit area, strategies A2-A4 return to being effective, i.e. $R_{134,137} < 1.0$.

Radiocesium migration within the soil column

Over time weathering of radiocesium within the soil column alters radiocesium profiles at undisturbed locations. Figs. 5a-d show how the slow migration of radiocesium down the soil column over time affects remediation residual dose factors if remediation parameters remain fixed.

The general trend of the results is for remediation performance to decrease with the elapsed time post-fallout. The faster the radiocesium migration within the soil column the higher the dependency of R_{134} and R_{137} on elapsed time. The rate of radiocesium migration observed by Likhtarev et al. (2002) is consistent with the slow radiocesium migration parameters from ICRU 53 (1994).

Amongst the remediation strategies, topsoil removal without recovering (A2) is most sensitive to the change in the initial activity distribution over time (Fig. 5b), while soil layer interchange (A3) is least sensitive (Fig. 5c). This effect is a consequence of the shallower remediation mass per unit area considered for topsoil removal (6.7 g cm^{-2}) than for soil layer interchange (40.3 g cm^{-2}). Migration of radiocesium down the soil column over time means that less of the radiocesium inventory is remediated by method A2 than method A3 under these fixed remediation masses per area.

One option to improve the performance of remediation method A2 would be to increase the remediation mass per unit area with elapsed time since fallout deposition. Similarly this option may be worth considering for topsoil removal with recovering (A1) and soil mixing (A4), where R_{134} and R_{137} also show a dependency on years elapsed since fallout, although to a lesser extent than strategy A2.

DISCUSSION

There are no discernible differences between the residual dose factors for ^{134}Cs and ^{137}Cs in Figs. 2-4. This result is a consequence of the similarity of the energies of the main gamma rays emitted by ^{134}Cs and ^{137}Cs upon decay. For ^{134}Cs these energies are 605 keV and 796 keV, and for ^{137}Cs, 662 keV.

Using this result, it is possible to combine Eqs. 1, 5 and 6 to give a formula for calculating the ambient dose equivalent rate after remediation from its initial value:

$$ {}_{\mathrm{r}}\dot{H}^*(10) = R \times [{}_{\mathrm{i}}\dot{H}^*(10) - {}^{\mathrm{nat}}{}_{\mathrm{i}}\dot{H}^*(10)] + {}^{\mathrm{nat}}{}_{\mathrm{r}}\dot{H}^*(10), \quad (8) $$

where $R = R_{137} \approx R_{134}$.

The concentration of natural radionuclides within soil is relatively constant and the source distribution of natural radionuclides will see little change due to remediation work. Therefore, the natural background component of the ambient dose equivalent rate will be unchanged by remediation work to a good approximation, i.e. ${}^{\mathrm{nat}}{}_{\mathrm{r}}\dot{H}^*(10) = {}^{\mathrm{nat}}{}_{\mathrm{i}}\dot{H}^*(10)$. Thus by interpolating R from Figs. 2-4 and employing Eq. 8, it is possible to calculate $\dot{H}^*(10)$ after remediation from its initial value and the natural background component for the simulated geometry.

The limitations of this study are as follows. The calculated residual dose factors strictly apply for the simulated geometry and detection location (open land, square remediation plots, dose rate at center of plot), and for the initial radioactivity distribution assumptions. The absolute magnitude of the residual dose factors will change with respect to different shape remediation plots or dose rate locations, but the general trend of the results in Figs. 2-4 is not expected to differ under variation of these factors. Simulations of this type are relatively inexpensive to perform on modern computers, so could be used to calculate applicable residual dose factors under different scenarios as required.

CONCLUSION

This study systematically evaluated residual dose factors for the radiocesium components of $\dot{H}^*(10)$ upon remediating open sites with fallout-contaminated soil. The size of the remediation area, the remediation mass depth and the initial depth distribution of the radioactivity were systematically varied to determine their effect on the results.

The topsoil removal strategies (A1 and A2) offer the benefit that radioactive cesium fallout can be removed from the remediation zone and isolated from the environment. The tendency for radiocesium to bind to clay minerals in soil means that the majority of the fallout is located in the top few centimeters of soil. Therefore stripping this topsoil can essentially clear the radiocesium from the remediated area. There is little benefit from a radiological perspective in recovering with a clean layer of shielding soil (A1) instead of leaving in the bare state (A2) if radiocesium has been removed from the remediation zone, as the residual dose rate after remediation is due to radiocesium lying outside the remediated area.

The soil layer interchange (A3) and the soil mixing (A4) strategies reduce ambient dose equivalent rates by redistributing radiocesium fallout deeper within the ground and exploiting

greater self-shielding of the radiocesium gamma rays by the soil. Layer interchange is more effective than mixing for a given remediation depth, as it redistributes the radio-cesium deeper within the ground. One factor not considered here but worthy of further investigation is having different thicknesses for the interchanged layers. This could prove more efficient that equal thickness layers.

Weathering causes radiocesium to migrate deeper within the soil column over time. As the initial radiocesium depth distribution affects the residual dose factors, it may be necessary to increase the remediation depth for strategies A1-A4 over time to maximize dose rate reductions within the remediation plot. The radiocesium depth distribution at a contaminated site prior to remediation can be established by taking soil cores and analyzing depth sections in a laboratory using gamma ray spectroscopy. Another option is to infer the distribution based on years elapsed post-fallout and published results from other contaminated areas (e.g. ICRU 1994; Likhtarev et al. 2002; Matsuda et al. 2015). Given the initial depth distribution, residual dose factors for different remediation scenarios can be obtained from the figures in this paper or by further bespoke modeling. The residual dose factors can then be used to gauge how the ambient dose equivalent rate will change upon remediation, and to determine remediation parameters that maximize dose rate reductions.

A main goal of remediation is to reduce annual effective doses to persons spending time within fallout contaminated areas. As the 1 m ambient dose equivalent rate provides a conservative estimate of the effective dose rate to people within environmental fields (Satoh et al. 2016), the yearly effective dose can be controlled and reduced using $\dot{H}^*(10)$, remediation and occupancy controls as necessary.

ACKNOWLEDGMENTS

We thank K. Saito for his advice on the manuscript. We acknowledge fruitful discussions with K. Miyahara and JAEA colleagues during this research. Calculations were performed on JAEA's BX900 supercomputer. We thank two anonymous reviewers for their helpful comments. This paper is dedicated to Monica Claudia O'Connor.

REFERENCES

Eckerman KF, Ryman JC. External exposure to radionuclides in air, water, and soil. U.S. Environmental Protection Agency; Federal Guidance Report No. 12; 1993.

EURANOS. Generic handbook for assisting in the management of contaminated food production systems in Europe following a radiological emergency. EURANOS(CAT1)-

TN(09)-03; 2010.

International Atomic Energy Agency. Environmental consequences of the Chernobyl accident and their remediation: 20 years of experience. STI/PUB/1239; 2008.

International Atomic Energy Agency. The Fukushima Daiichi accident: technical volume 5/5 – post-accident recovery. STI/PUB/1710; 2015.

International Commission on Radiation Units and Measurements. Quantities and Units in Radiation Protection and Dosimetry. Bethesda, MD; ICRU Report 51; 1993.

International Commission on Radiation Units and Measurements. Gamma-ray spectrometry in the environment. Bethesda, MD; ICRU Report 53; 1994.

International Commission on Radiological Protection. ICRP Publication 103: The 2007 Recommendations of the International Commission on Radiological Protection. Ann. ICRP 37:1-332; 2007. DOI:10.1016/j.icrp.2007.10.001

International Commission on Radiological Protection. ICRP Publication 111: Application of the Commission's Recommendations to the Protection of People Living in Long-term Contaminated Areas after a Nuclear Accident or a Radiation Emergency. Ann. ICRP 39:1-67; 2009. DOI:10.1016/j.icrp.2009.09.002

Jacob P, Fesenko S, Firsakova SK, Likhtarev IA, Schotola C, Alexakhin RM, Zhuchenko YM, Kovgan L, Sanzharova NI, Ageyets V. Remediation strategies for rural territories contaminated by the Chernobyl accident. J Environ Radioact 56:51-76; 2001. DOI:10.1016/S0265-931X(01)00047-9

Jacob P, Fesenko S, Bogdevitch I, Kashparov V, Sanzharova N, Grebenshikova N, Isamov N, Lazarev N, Panov A, Ulanovsky A, Zhuchenko Y, Zhurba, M. Rural areas affected by the Chernobyl accident: Radiation exposure and remediation strategies. Sci Total Environ 408:14–25; 2009. DOI:10.1016/j.scitotenv.2009.09.006

Japan Atomic Energy Agency (JAEA). Remediation of contaminated areas in the aftermath of the accident at the Fukushima Daiichi Nuclear Power Station: Overview, analysis and lessons learned part 1: A report on the "Decontamination Pilot Project". JAEA-Review 2014-051; 2015. DOI:10.11484/jaea-review-2014-051

Likhtarev IA, Kovgan LN, Jacob P, Anspaugh LR. Chernobyl accident: retrospective and prospective estimates of external dose of the population of Ukraine. Health Phys 82:290-303; 2002. DOI:10.1097/00004032-200203000-00002

Malins A, Okumura M, Machida M, Takemiya H, Saito K. Fields of View for Environmental Radioactivity. In: Proceedings of the International Symposium on Radiological Issues for Fukushima's Revitalized Future. Fukushima, Japan; 2015: 28-34.

Malins A, Kurikami H, Nakama S, Saito T, Okumura M, Machida M, Kitamura A. Evaluation of ambient dose equivalent rates influenced by vertical and horizontal distribution of radioactive cesium in soil in Fukushima Prefecture. J Environ Radioact 151:38-49; 2016. DOI:10.1016/j.jenvrad.2015.09.014

Matsuda N, Mikami S, Shimoura S, Takahashi J, Nakano M, Shimada K, Uno K, Hagiwara S, Saito K. Depth profiles of radioactive cesium in soil using a scraper plate over a wide area surrounding the Fukushima Dai-ichi Nuclear Power Plant, Japan. J Environ Radioact 139:427-434; 2015. DOI:10.1016/j.jenvrad.2014.10.001

Okumura M, Nakamura H, Machida M. Mechanism of strong affinity of clay minerals to radioactive cesium: first-principles calculation study for adsorption of cesium at frayed edge sites in muscovite. J Phys Soc Jpn 82:033802; 2013. DOI:10.7566/JPSJ.82.033802

Saito K, Petoussi-Henss N. Ambient dose equivalent conversion coefficients for radionuclides exponentially distributed in the ground. J Nucl Sci Technol 51:1274-1287; 2014. DOI:10.1080/00223131.2014.919885

Sato T, Niita K, Matsuda N, Hashimoto S, Iwamoto Y, Noda S, Ogawa T, Iwase H, Nakashima H, Fukahori T, Okumura K, Kai T, Chiba S, Furuta T, Sihver L. Particle and heavy ion transport code system, PHITS, version 2.52. J Nucl Sci Technol 50:913-923; 2013. DOI:10.1080/00223131.2013.814553

Satoh D, Furuta T, Takahashi F, Endo A, Lee C, Bolch WE. Age-dependent dose conversion coefficients for external exposure to radioactive cesium in soil. J Nucl Sci Technol 53:69-81; 2016. DOI:10.1080/00223131.2015.1021286

Ulanovsky A, Jacob P, Fesenko S, Bogdevitch I, Kashparov V, Sanzharova N. ReSCA: Decision support tool for remediation planning after the Chernobyl accident. Radiat Environ Biophys 50:67-83; 2011. DOI:10.1007/s00411-010-0344-7

United Nations Scientific Committee on the Effects of Atomic Radiation. Sources, effects and risks of ionizing radiation, UNSCEAR 2013 report, Volume I: Levels and effects of radiation exposure due to the nuclear accident after the 2011 great east-Japan earthquake and tsunami. 2014.

Yasutaka T, Naito W, Nakanishi J. Cost and effectiveness of decontamination strategies in radiation contaminated areas in Fukushima in regard to external radiation dose. PLoS ONE 8:e75308; 2013. DOI:10.1371/journal.pone.0075308

Yasutaka T, Naito W. Assessing cost and effectiveness of radiation decontamination in Fukushima Prefecture, Japan. J Environ Radioact 151:512-520; 2016. DOI:10.1016/j.jenvrad.2015.05.012

Table 1. Typical ranges of remediation depths and remediation masses per unit area for the different remediation strategies. Ranges of remediation depths from JAEA (2015). The remediation masses per unit area were calculated from these assuming soil with constant density 1.35 g cm^{-3}, based on the densities of soil samples from Fukushima Prefecture, Japan (Malins et al. 2016).

	Strategy	Remediation depth (cm)	Remediation mass per area (g cm^{-2})
A1	Topsoil stripping followed by recovering	2-5	2.70-6.75
A2	Topsoil stripping only	2-5	2.70-6.75
A3	Position interchange of topsoil and subsoil layers	30-45	40.50-60.75
A4	Mixing the topsoil down to a fixed depth	25-50	33.75-67.50

Table 2. Indicative values of relaxation mass per unit area for radiocesium at undisturbed grassland sites for moderate climates, as a function of years since fallout deposition from ICRU 53 (ICRU 1994).

Elapsed time (y)	Relaxation mass per area (g cm^{-2})
0-1*	1.0
1-5	3.0
5-20	10.0

* Precipitation ≥ 3.0 mm.

Table 3. Years elapsed since fallout, attenuation factors (r_{Cs}) using parameters from Likhtarev et al. (Likhtarev et al. 2002), and corresponding relaxation masses per unit area (β) for the exponential distribution.

Time elapsed (y)	Attenuation factor	Relaxation mass per area (g cm^{-2})
2	0.609	1.33
3	0.554	1.91
4	0.517	2.41
5	0.492	2.83
6	0.473	3.18
7	0.459	3.47
8	0.448	3.71
9	0.439	3.92
10	0.432	4.12
11	0.424	4.31
12	0.418	4.49
13	0.412	4.67

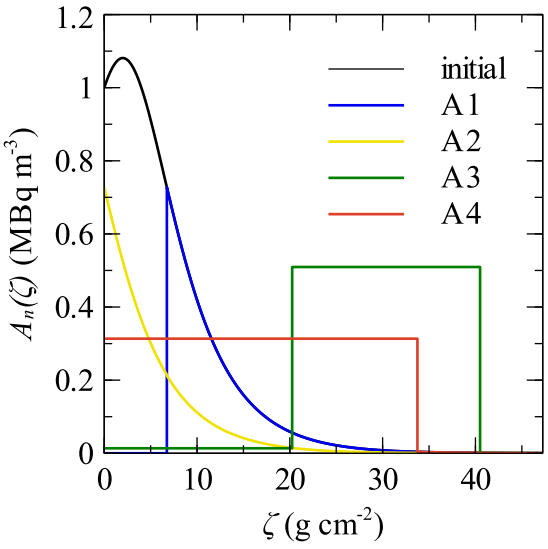

Fig. 1. Idealized activity distributions of radiocesium within soil used to calculate the change in $\dot{H}^*(10)$ by remediation. The black line is an initial distribution prior to remediation (hyperbolic secant function with $A_{n,0}$ = 1.0 MBq m^{-3}, β = 5.0 g cm^{-2} and ζ_0 = 2.0 g cm^{-2} – Eq. 4). The colored lines show post-remediation distributions for each of strategies A1-A4.

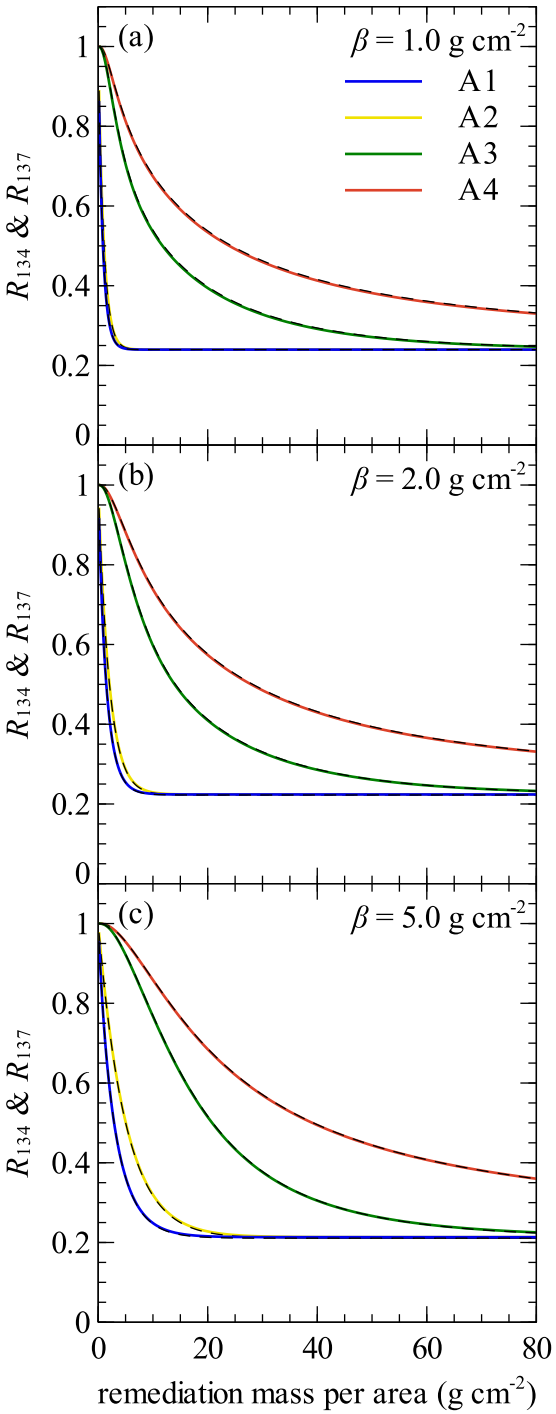

Fig. 2. The residual components of $^{134,137}\dot{H}^*(10)$ after remediation relative to the prior value (residual dose factors) for strategies A1-A4 as a function of the remediation mass per unit area. The results are for an initial activity distribution which is exponential as a function of mass depth. The square remediation plot is 37.5 by 37.5 m. Colored lines indicate results for ^{137}Cs, while dashed lines are corresponding results for ^{134}Cs. Panels (a) to (c) show the effect of β in the initial exponential distribution.

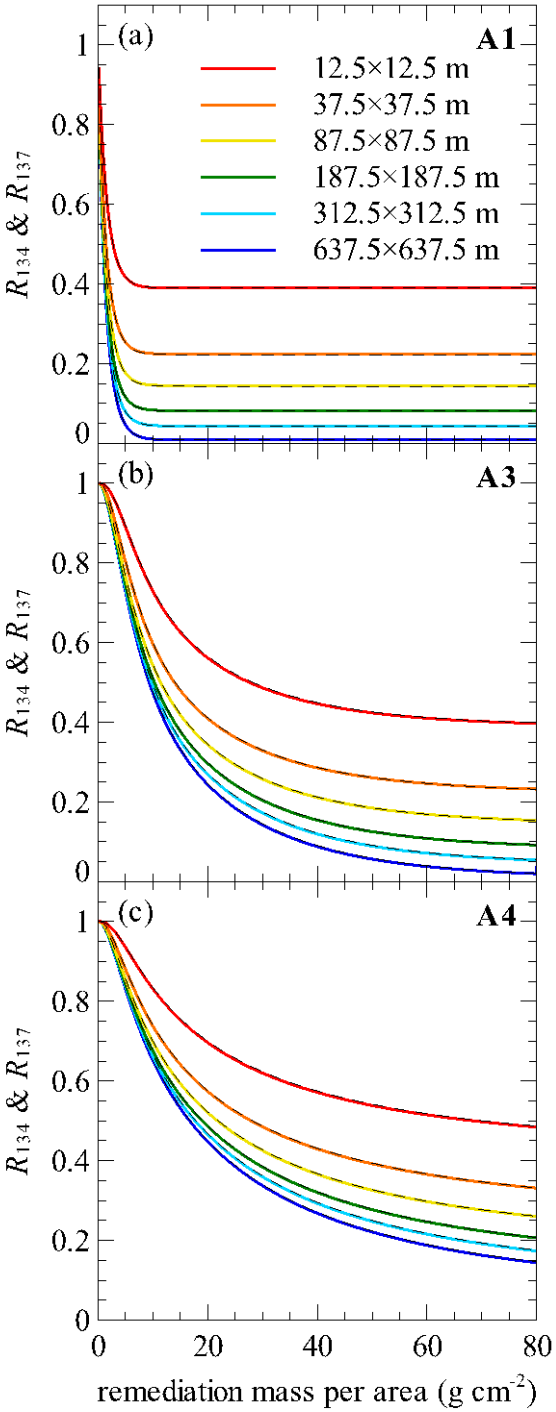

Fig. 3. The effect of the area of remediated land on residual dose factors. Colored lines represent different sizes of the square remediation plot (^{137}Cs fallout). Corresponding dashed lines show results for ^{134}Cs. Initial radiocesium distribution within soil is exponential with β = 2.0 g cm^{-2}. Panel (a) shows results for topsoil stripping and recovering with clean soil (A1), (b) for soil layer interchange (A3), and (c) results for topsoil mixing (A4).

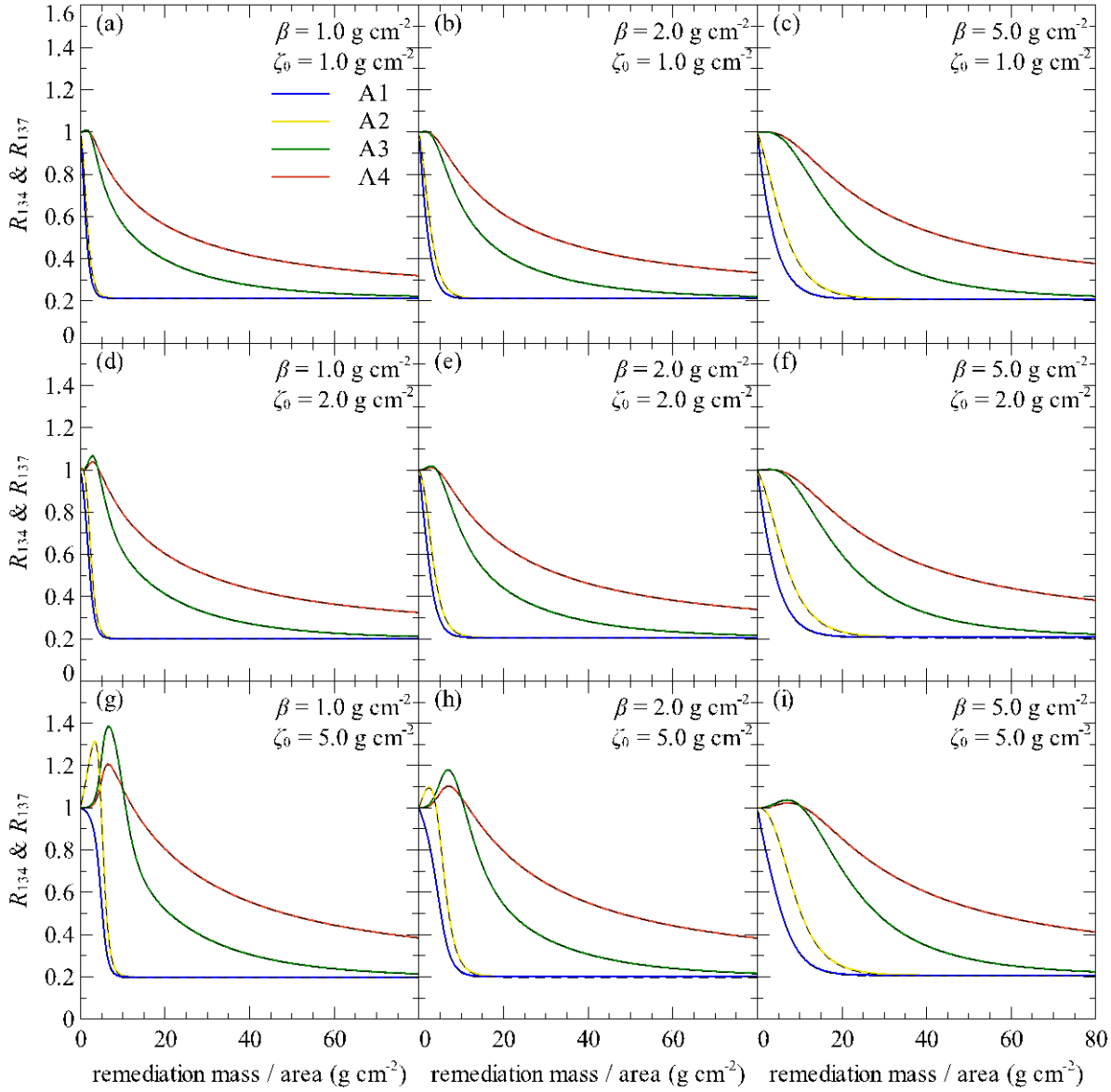

Fig. 4. Residual dose factors as functions of the remediation mass per unit area given for different initial hyperbolic secant activity distributions. Meaning of line colors and styles as per Figs. 2a-c. The square remediation plot is 37.5 by 37.5 m. β in the hyperbolic secant distribution increases between the panels from left to right; ζ_0 increases between panels from top to bottom.

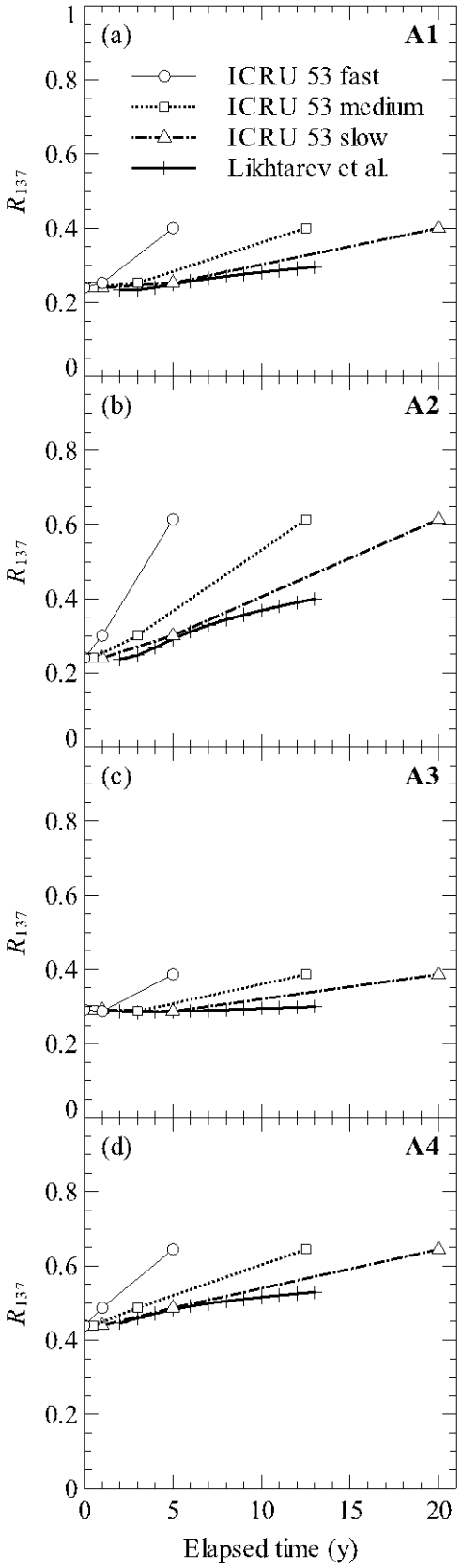

Fig. 5. Effect of radiocesium migration down the soil column in years following fallout deposition on the residual dose factor R_{137} if remediation parameters remain fixed. Radiocesium migration downwards means remediation becomes more difficult over time.